Supplementary Information

Deconvoluting the electronic landscape of ZnO using 2D excitation-emission spectroscopy: effects of microstructuring, doping and restructuring

*Daniel J. Oliver[a], Victor V. Volkov[a] and Carole C. Perry**
Interdisciplinary Biomedical Research Centre, School of Science and Technology, Nottingham Trent University, Clifton Lane, Nottingham NG11 8NS, United Kingdom.
[a] contributed equally
Corresponding author: carole.perry@ntu.ac.uk

Materials and Methods

Chemical Materials

Sodium citrate ($Na_3C_6H_5O_7$), 1,3-hexamethylenetetramine (HMTA, $C_6H_{12}N_4$) was from Sigma-Aldrich (St. Louis, Missouri USA). Zinc nitrate hexahydrate ($Zn(NO_3)_2{\cdot}6H_2O$) was purchased from Honeywell Fluka, Thermo Fisher Scientific Inc.(Charlotte, North Carolina USA). All these materials were used without any further treatment. If required, type 1 water was used with a resistance of 18 MΩ at 25 °C.

Polypolypeptide Synthesis and Characterization

GT16 polypolypeptide (GLHVMHKVAPPRGGGC) was purchased from Pepceuticals (Leicester, UK). Synthesis of the ZA2 polypolypeptide (GLHVMHKVAYSSGAPPMPPF) was reported previously.[1,2]

Zinc oxide samples

The **analytical standard** material was purchased from Sigma-Aldrich (St. Louis, Missouri USA) and used without further modification. All other ZnO samples were prepared using HMTA and sodium citrate. **ZnO polycrystalline microspheres** were synthesised as reported previously:[3] in brief, a reaction mixture (10 ml) containing 50 mM $Zn(NO_3)_2$, 50 mM HMTA and 38 mM sodium citrate was prepared and mixed at room temperature. The solution was heated to 90°C for 1.5 hours and the precipitate formed collected by centrifugation using Centrifuge 5904R M (Eppendorf SE, Hamburg, Germany) at 5000 rpm for 5 minutes. The pellet was washed with 2x 10ml Type-I water, 1x 10ml absolute EtOH before being suspended in 500µL Type-I water and immediately lyophilised. **Zinc oxide nanorods** were synthesized using a procedure documented in the literature[1,4] using HMTA (0.42g, Sigma-Aldrich), $Zn(NO_3)_2{\cdot}6H_2O$ 0.058g (Honeywell Fluka, Thermo Fisher Scientific Inc., Charlotte, North Carolina USA) & 18mΩ H_2O (90mL) placed into a glass reaction vessel. The reaction mixture was incubated at 20 °C using a water bath stirrer setup for 24 hours. Subsequently, the samples were incubated at 68 °C using a water bath stirrer setup for a further 48 hours. Post incubation the precipitate was separated from the reaction medium using centrifugation (10 mins, 13000 rpm) using a Centrifuge 5804 R (Eppendorf SE, Hamburg, Germany) and washed with 18MΩ H_2O three times before being lyophilised.

Polypeptide Mediated Zinc Oxide Synthesis

ZnO platelets and nanoflowers were prepared using a procedure documented in the literature,[1,4,5] using GT16 and ZA2 polypeptide, respectively (2.82mM, 1mL), HMTA (0.42g, Sigma-Aldrich), $Zn(NO_3)_2{\cdot}6H_2O$ 0.058g (Honeywell Fluka, Thermo Fisher Scientific Inc., Charlotte, North Carolina USA) & 18MΩ H_2O (89mL) placed into a glass reaction vessel. The reaction mixture was incubated at 20 °C using a water bath stirrer setup for 24 hours. Subsequently, the samples were incubated at 68 °C using a water bath stirrer setup for a further 48 hours. Post incubation the precipitate was separated from the reaction medium using centrifugation (10 mins, 13000 rpm) using a Centrifuge 5804 R (Eppendorf SE, Hamburg, Germany) and washed with 18mΩ H_2O three times before being lyophilised. The **ZnO-polypeptide-Au composite** one-pot synthesis route used peptide ZA2 engineered from regions of G12 (a known ZnO binder and parent polypeptide of GT-16[2]) and A3 (a known and well-studied Au binder).[6]

Utilising the novel ZA2 sequence and a modification to a procedure documented in the literature,[1,4] ZnO-ZA2-Au nanocomposite materials were prepared using $HAuCl_4$ (10 mM, 9 ml, Sigma), ZA2 Polypeptide (GLHVMHKVAYSSGAPPMPPF, 2.82mM, 1mL), HMTA (0.42g, Sigma-Aldrich), $Zn(NO_3)_2{\cdot}6H_2O$ 0.058g (Honeywell Fluka, Thermo Fisher Scientific Inc., Charlotte, North Carolina USA) & 18mΩ H_2O (80mL) placed into a glass reaction vessel. The reaction mixture was incubated at 20 °C using a water bath stirrer setup for 24 hours. Subsequently, the samples were incubated at 68 °C using a water bath stirrer setup for a further 48 hours. Post incubation the precipitate was separated from the reaction medium using centrifugation (10 mins, 13000 rpm) using a Centrifuge 5804 R (Eppendorf SE, Hamburg, Germany) and washed with 18mΩ H_2O three times before being lyophilised.

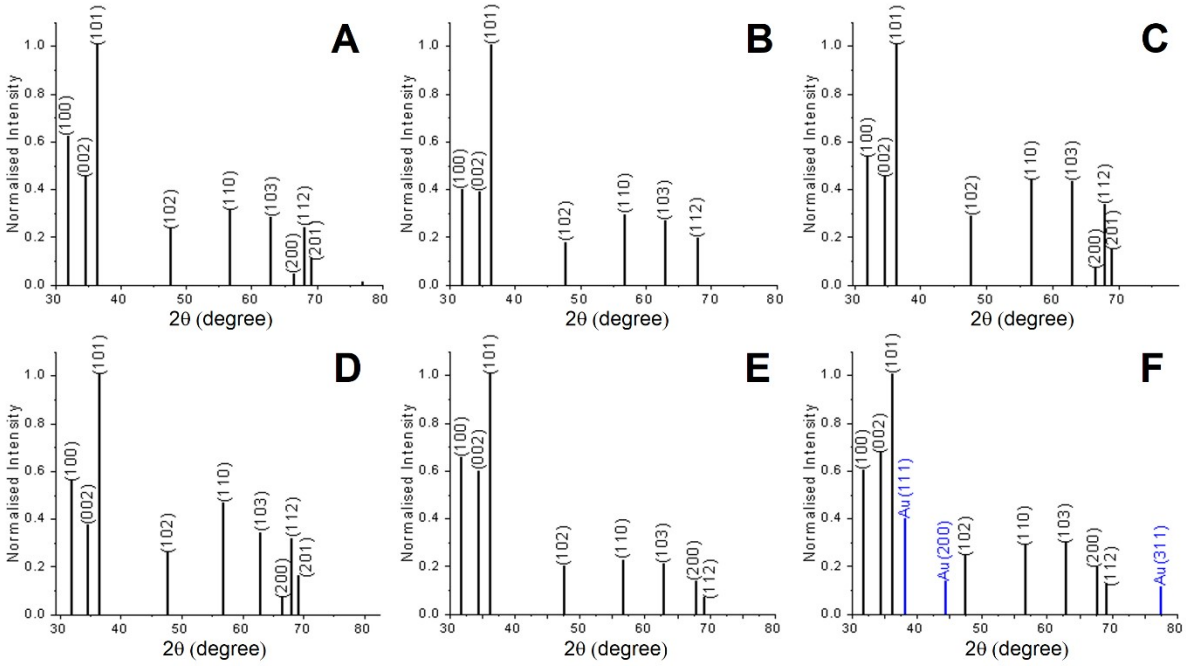

Figure S1. *X-ray for pure ZnO analytical standard (A), microspheres (B), nanorods (C); and for hybrid nanoplatelets (D), nanoflowers (E), ZnO-ZA2-Au nanocomposite (F).*

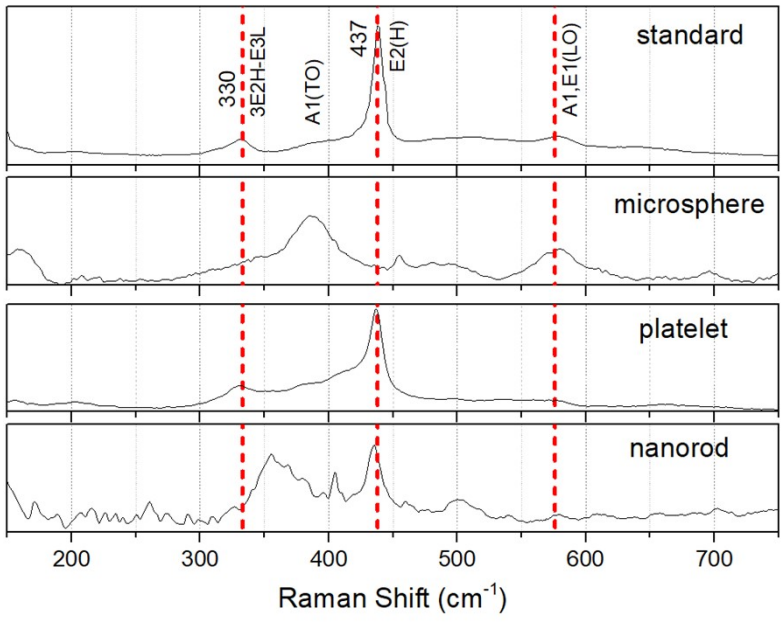

Figure S2. *Raman spectra ZnO analytical standard, microspheres, nanoplatelets and nanorods, as indicated.*

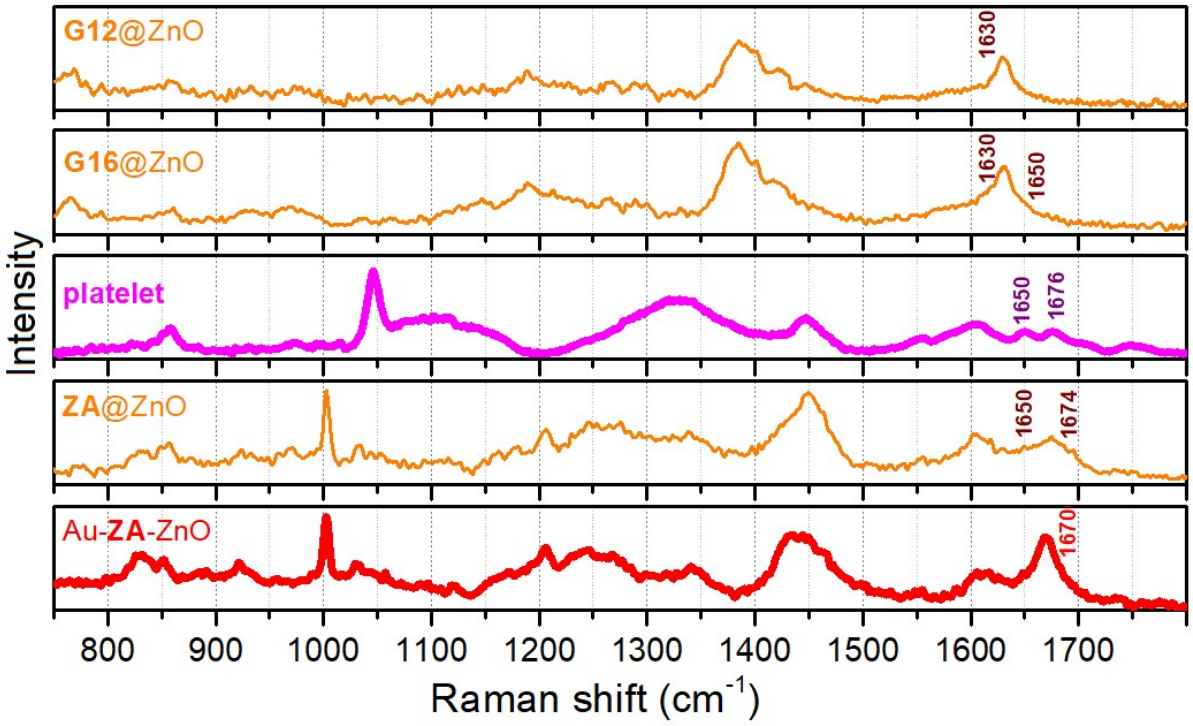

Figure S3. *Raman spectra of G12, G16, and ZA polypeptides when at surface of ZnO analytical standard (orange line), as well as Raman spectra for platelet and Zu-ZA-ZnO hybrid systems, as indicated.*

Fitting of two-dimensional excitation-emission spectra

Figures S4-S6 compare 2D spectra of the considered ZnO structures as prepared and after PVA and NaBH4 treatments, respectively and their fits according to the procedure we reported previously.[7]

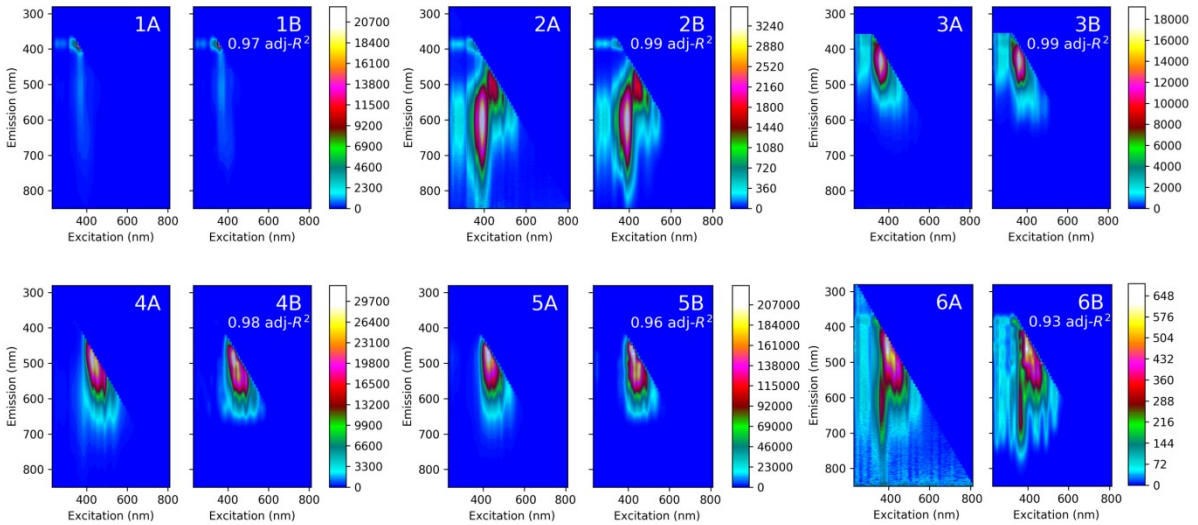

Figure S4. *2D spectra of the ZnO library explored and their respective fits with the adj-R2 value reported. Where: A' denotes the experimental data and 'B' denotes the proposed model. The numbers denote: 1) analytical standard, 2) nanorods, 3) microspheres, 4) nanoplatelets, 5) nanoflowers, 6) ZnO-Au composite. The color bar shown on the right of each figure is for the experimental data plot 'A' and is representative of the color bar of plot 'B'.*

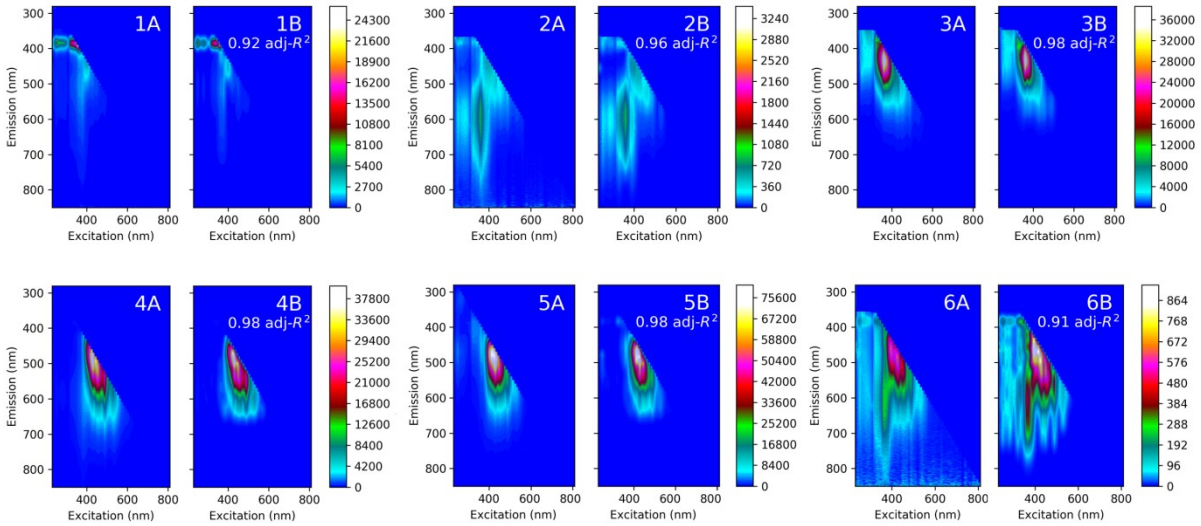

Figure S5. *2D spectra of the 0.5% PVA treated ZnO library explored and their respective fits with the adj-R2 value reported. Where: A' denotes the experimental data and 'B' denotes the proposed model. The numbers denote: 1) analytical standard, 2) nanorods, 3) microspheres, 4) nanoplatelets, 5) nanoflowers and 6) ZnO-Au composite. The color bar shown on the right of each figure is for the experimental data plot 'A' and is representative of the color bar of plot 'B'.*

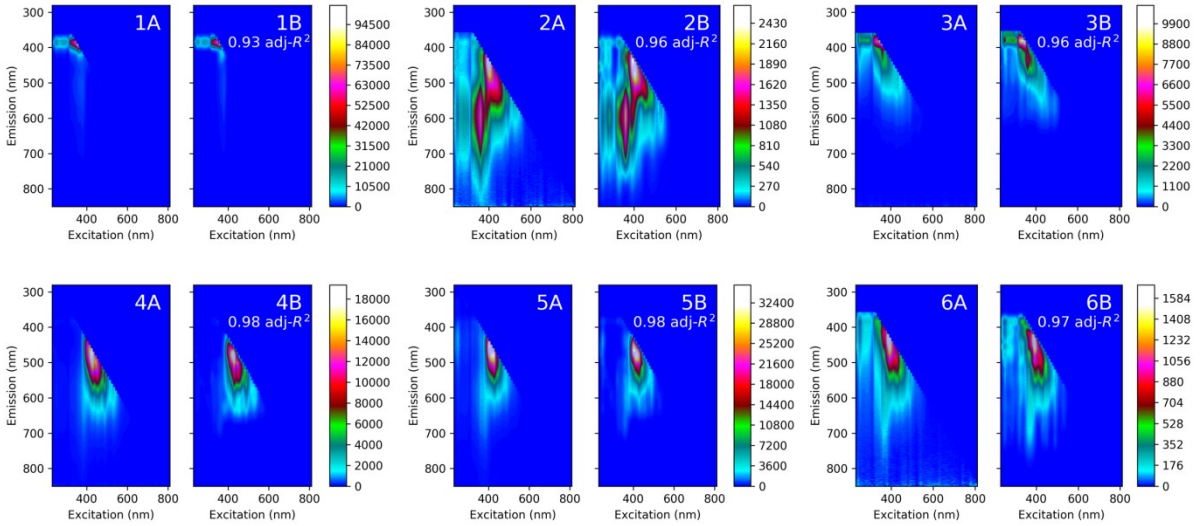

Figure S6. *2D spectra of the 1M $NaBH_4$ treated ZnO library explored and their respective fits with the adj-R2 value reported. Where: A' denotes the experimental data and 'B' denotes the proposed model. The numbers denote: 1) analytical standard, 2) nanorods, 3) microspheres, 4) nanoplatelets, 5) nanoflowers, and 6) ZnO-Au composite. The color bar shown on the right of each figure is for the experimental data plot 'A' and is representative of the color bar of plot 'B'.*

Assignment of acceptor and donor states based on literature precedence.

Considering distributions of spectral components along the diagonal for the considered systems, we sort detected emission spectra into five groups, according to excitation wavelengths. The first "exciton and near band gap" group accounts relaxation involving band-gap and closely associated states that are excited when we use radiation with wavelength in the spectral range from 330 to 370 nm. The second "ultraviolet excitation" group of transitions is excited using radiation in the spectral range from 370 to 410 nm. As one may find exploring 2DEM spectra in Figure S7, this set gives rise to the "yellow-red" emission in nanorods. We observe the third and the fourth "blue excitation" and "green

excitation" sets excited in the spectral range from 410 to 440 nm and from 440 to 480 nm, respectively,

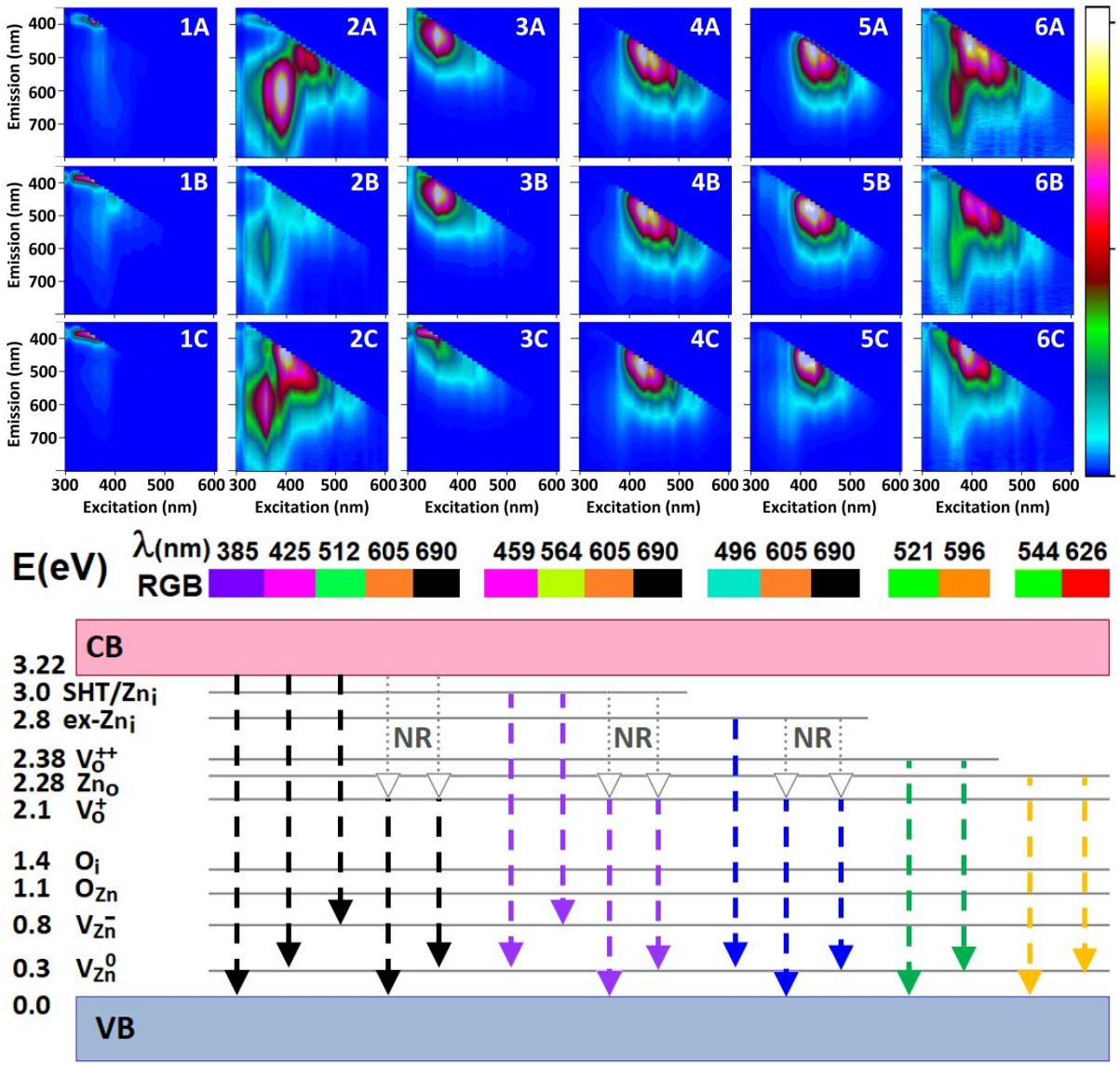

Figure S7. ***Upper set:*** *2D excitation-emission data sets for the ZnO library (A), 0.5% PVA treated (B) and 1M $NaBH_4$ treated (C). The numbers denote: 1) analytical standard, 2) nanorods, 3) microspheres, 4) nanoplatelets, 5) nanoflowers & 6) ZnO-ZA2-Au composite.* ***Lower set:*** *Energy relaxation diagram we generalise according to our fitting[7] to account emissive components specific to Band Gap/Exciton, ultraviolet, blue, green and yellow excited groups of emission and non-radiative (NR) relaxation, as observed in the considered ZnO based microstructures: Discussion in the main text provides further specifications*.

to yield relatively effective "green" emission in nanorods and hybrid systems. The fifth excitation group, excited in the spectral range from 480 to 560 nm, is a relatively low yield "yellow excitation" emissive sub-set. Following fitting[7] of the experimental 2DEM data we may compare with literature for assignment of likely donor and acceptor states.

Band Gap and Exciton emission

For ZnO with wurtzite symmetry, theoretical analysis[8] of magneto-optic exciton fine structure experimental data[9] confirmed Γ_7 symmetry of the band splitting (with E_g = 3.4376 at T = 4.2K) by crystal

field and spin-orbit interactions that promotes free exciton emission at about 3.377 eV.[10] This emission includes ionised donor bound and neutral donor bound contributions at 3.367 eV within the energy range between 3.3628 and 3.359 eV, respectively.[11] Considering this and results of the temperature effect for ZnO sheets;[12] for the analytical standard, we may assign the dominant UV emission maximum at 384±3 nm (3.22±0.03 eV) with excitation most effective at 370 nm (3.35 eV): see Figure S7(1A), and the result of fitting as red arrows in Figure S8A. Accordingly, we introduce the free exciton signature of the conducting band (CB) to be 3.22 eV above the valence band (VB). Here, the value of resonance energy is according to temperature dependent broadening and fitting uncertainty.

Heterogeneity of "UV excited" "blue" emissions

Next, we consider excitation at 370 nm (3.35 eV). Below the exciton emission, we detect luminescence with the maximum at about 425±10 nm. At the same time, when shifting excitation to longer wavelength at 400 nm, we detect a highest energy emission peak at about 459±20 nm. Both "blue" emissions are relatively weak in the case of the analytical standard sample, but are obvious in the 2D spectrum of the microsphere sample: see the spectrum Figure S7(1B) and the result of fitting as black arrows in Figure S8A. The dominance of these components makes the microsphere sample rather unique. Here we stress that using the 2D presentation format allows one to make a secure numerical factoring of these different "blue" emissive components possible. When using conventional spectroscopy such is difficult: for example, one may consider the inhomogeneous band at about 2.96 eV as reported in ZnO sheets.[12] While we explore 2D spectra detected at room temperature, we may expect that a low temperature experiment would be helpful to resolve the manifold of "blue" emissions[13] better.

To model the "blue" emissive components at 425±10 nm and 459±20 nm while under 370 nm and 400 nm excitations, respectively, we introduce 0.3 eV and 3.0 eV donor and acceptor state (the energies are in respect to VB) to provide the transitions E(3.22 eV)→E(0.3 eV) and E(3.0 eV)→E(0.3 eV) at the wavelengths to fit the observed data. Based on early experimental assignments,[14] and later theoretical studies[15,16] we consider the zero charge Zn vacancy as the deep acceptor (V_{Zn}^0) that participates in the higher energy "blue" emission. Concerning the other transition: we may consider the state E (3.0 eV) to present shallow traps and Zn interstitial defects (Zn_i).[16-18] According to results of infrared[19,20] and electron nuclear double resonance (ENDOR) experiments,[21] hydrogen donors, including those present as -OH groups are expected to contribute to the density of shallow traps in ZnO.[21,22]

Assignment of the "yellow excited" group of emissions

For all ZnO containing samples explored in this study, fitting[7] of the 2D spectral components excited using light in the spectral range 480-560 nm, suggests two weak contributions at about 544±20 nm and 626±20 nm: see Figure S8B. Such transitions are particularly obvious in 2D spectra detected for hybrid ZnO systems prepared in the presence of peptidic material: see Figure S7 (4A-6A). Considering the excitation wavelength range is well below the CB, in order to explain the observed transitions, we introduce a donor state at about 2.28 eV to yield E(2.28 eV)→E(0 eV) and E(2.28 eV)→E(0.3 eV) transitions at about 544±20 nm and 626±20 nm, respectively. The detected emissions are of weak intensity suggesting a low probability of the corresponding donor states. Based on computed formation energies and relative order if levels in respect to the CB and VB,[16] we ascribe donor zinc anti-sites (Zn_O) as leading to the weak "green yellow" Zn_O →VB and "deep red" Zn_O → V_{Zn}^0 transitions at about 544±20 nm and 626±20 nm, respectively.

Assignment of the "green excited" group of emissive transitions

At this point, before we review the main emission subset (excited in UV sets 1 and 2), it is convenient to address and assign transitions of the lower energy manifold. The 2D spectral emission subset

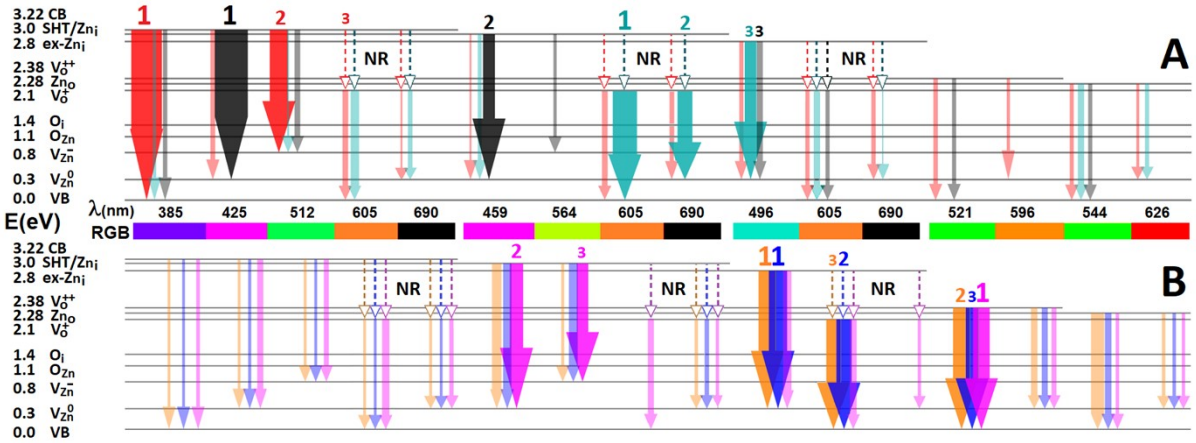

Figure S8. ***Panel A:*** *energy relaxation in pure ZnO materials: analytical standard (red), microsphere (black) and nanorod (cyan).* ***Panel B:*** *energy relaxation in hybrid ZnO systems: nanoplatelet (orange), nanoflower (blue) and Au including microstructure (magenta). Thickness of arrows is proportional to quantum yields, computed using 2D fitting protocol.[7] Numbers 1, 2 and 3 indicate leading, next and third relaxation pathway for the corresponding material according to color. We fade colors for weaker transitions. NR corresponds to non-radiative relaxation.*

corresponds to excitation in the spectral range 440-480 nm. Fitting 2D line-shapes[7] leads to two transitions at 521 and 596±20 nm, which are particularly intense in the hybrid systems: see Figure S8B. Since both wavelengths are relatively blue shifted (comparing with those of the emission specific to the "yellow excited" set) we may discard a possible role of non-radiative relaxation to the lower (according to our placement) Zn_O level. To model the observed transitions under the indicated in-gap excitation, we introduce an emitting state at about 2.38 eV above the VB.

A significant number of experimental[23-28] studies suggest a role of oxygen vacancies, to explain such transitions. Based on theoretical insights,[16,29,30] and results of time-resolved X-ray spectroscopy,[31] we assign the donor state at about 2.38 eV (above VB) to oxygen vacancies (V_O^{++}) to provide the fitted 2D emission components at about 521 and 596±20 nm along the V_O^{++}→VB and V_O^{++} → V_{Zn}^0 relaxation pathways, respectively: see Figure S8.

Assignment of the "blue excited" group of emissive states

Having the lower acceptor part of the ladder manifold addressed, we review emissive transitions excited in the range from 410 to 440 nm. Fitting 2D spectra reveals three emissive components at about 496, 605 and 690±20 nm. Considering the excitation wavelength range (therefore, the attainable energy above the VB); to model the first component we may introduce an emissive state at 2.8 eV, which we may ascribe to extended zinc interstitial defects (ex-Zn_i).[24] Accordingly, transitions ex-Zn_i → V_{Zn}^0 would have a wavelength consistent with that observed at 496 nm. This transition is the main energy relaxation pathway for nanoplatelet and nanoflower hybrid systems: see Figure S8B.

To address the other two transitions, here, it is important to note, that experimental steady state spectroscopy[23] as well as time-resolved photoluminescence studies[32] reported an effective non-radiative relaxation to oxygen vacancies to provide a consequent "green" and relevant emission components. Accounting the reported interactions of V_O^{++} and V_O^{+} vacancies as reported by time resolved X-ray spectroscopy,[31] and the computed energy levels for the vacant orbital components of the of the V_O^{+} vacancy, we ascribe the 605 and 690±20 nm emissions to V_O^{+} → VB and V_O^{+} → V_{Zn}^0 transitions, respectively.

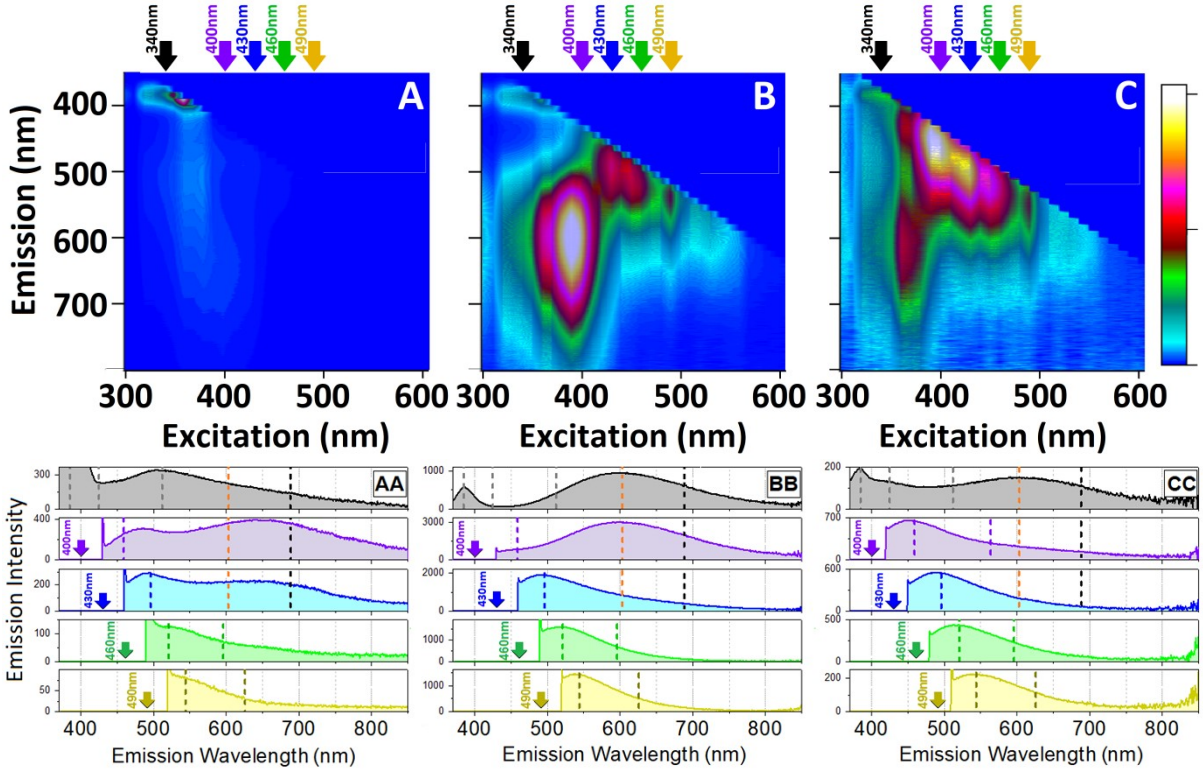

Figure S9. *Demonstration of 2D fitting[7] capacity. Upper set of panels: 2D spectra of analytical standard (A), nanorods (B), and ZnO-ZA2-Au composites (C) with arrows to indicate excitations of "exciton and near band gap", "ultraviolet", "blue", "green" and "yellow" excited sets, as we name them. Lower set of panels: the corresponding 1D slices from 2D spectra of analytical standard (AA), nanorods (BB), and ZnO-ZA2-Au composites (CC). The vertical dashed lines indicate positions of band wavelengths according to fitting of 2D spectra, while the dashed orange and black lines indicate positions of fitted components we ascribe to V_o^+ state after a non-radiative decay from an upper excited state.*

Assignment of "ultraviolet excited" emissions

Using the 2D fitting procedure,[7] we can define that excited in the UV spectra range from 370 to 410 nm, the 2D spectra comprises four emissive components at 459, 564, 605 and 690±20 nm. The blue component at 459 nm we have addressed already, while reviewing heterogeneity of the "blue" emissions. The transition at about 564 nm we ascribe to shallow trap (SHT) → V_{Zn}^- and/or to Zn_i → V_{Zn}^- transitions. The red and the near infrared transitions are the non-radiative mediated relaxations V_O^+ → VB and V_O^+ → V_{Zn}^0, respectively.

Assignment of exciton and near band gap emission

We complete the review of ZnO band gap specific ladder of states returning to emissions excited using the most energetic radiation in the spectral range from 330 to 370 nm. In this excitation region, 2D fitting suggests luminescence bands at 385, 425, 512, 605, and 690 nm. As we discussed previously, the first component and the second components are the exciton and the CB→ V_{Zn}^0 emissions, respectively, while the red and the near infrared emissions are due to non-radiative mediated V_O^+ contributions. 2D spectra and their fitting demonstrate, that under ultraviolet excitation, the "green" spectral component at 512±20 nm is rather distinct and the second most dominant in the analytical standard. At the same time, 2D spectra indicate that such emission does not play any significant role in other samples studied here. Accounting for the relatively low quantum yield of this emission, we assign it to CB → V_{Zn}^- transition.

From the above discussion we show that 2D excitation emission spectra do not allow a discussion on a unique source of a "green", or "blue", "red" emission, which is typical in studies using conventional

spectroscopy. Instead, the approach allows unambiguous specification how the ZnO energy manifold may sustain pathways under different excitations to yield emissions of similar colors. As a consequence, we demonstrate that ZnO may emit similar color “green” or “blue” emissions due to different relaxation pathways under different excitations. The two-dimensional spectroscopy approach allows factoring such contributions. Furthermore, fitting 2D spectra we may review and compare energy relaxation diagrams for different ZnO systems and explore the effect of external perturbations, as we present in Figure S8 and in Figures 3-5 in the main text.

According to the slice examples in Figure S9, one may clearly see that if we would conduct fitting of 1D spectra separately, we would not be able to reproduce wavelengths of transitions as suggested by 2D fitting. This is because, due to the spectral width of any selected excitation, a 1D spectrum is expected to account contributions of neighbouring (along the excitation axis) pathways. Fitting 2D spectra does allow one to account for this issue.

REFERENCES

1. M.-K. Liang, M. J. Limo, A. Sola-Rabada, M. J. Roe and C. C. Perry, *Chem. Mater.*, 2014, **26**, 4119.
2. M.-K. Liang, O. Deschaume, S. V. Patwardhan and C. C. Perry, *J. Mater. Chem.*, 2011, **21**, 80.
3. V. V. Volkov, D. J. Oliver and C. C. Perry, *Nat. Comm.*, 2020, **11**, 4908.
4. M. J. Limo and C. C. Perry, *Langmuir*, 2015, **31**, 6814.
5. M. M. Tomczak, M. K. Gupta, L. F. Drummy, S. M. Rozenzhak and R. R. Naik, *Acta Biomater.*, 2009, **5**, 876.
6. J. M. Slocik, M. O. Stone and R. R. Naik, *Small*, 2005, **1**, 1048.
7. D. J. Oliver, V. V. Volkov and C. C. Perry, *Adv. Mater. Interfaces*, 2022, **10**, 2202048.
8. W. L. R. Lambrecht, *Phys. Rev.* B, 2002, **65**, 075207.
9. B. Gil, *Phys. Rev. B*, 2001, **64**, 201310 (R).
10. B. K. Meyer, H. Alves, D. M. Hofmann, W. Kriegseis, D. Forster, F. Bertram, J. Christen, A. Hoffmann, M. Straßburg, M. Dworzak, U. Haboeck and A. V. Rodina, *Phys. Status Solidi B*, 2004, 241, 231.
11. D. C. Reynolds, C. W. Litton and T. C. Collins, *Phys. Rev.*, 1965, **140**, A1726.
12. H. He, Y. Wang, J. Wanga and Z. Ye, *Phys. Chem. Chem. Phys.*, 2011, **13**, 14902.
13. F. Kayaci, S. Vempati, I. Donmez, N. Biyikli and T. Uyar, *Nanoscale*, 2014, **6**, 10224.
14. B. Lin, Z. Fu and Y. Jia, *Appl. Phys. Lett.*, 2001, **79**, 943.
15. A. Janotti and C. G. Van de Walle, *Phys. Rev. B*, 2007, **76**, 165202.
16. F. Oba, M. Choi, A. Togo and I. Tanaka, *Sci. Technol. Adv. Mater.*, 2011, **12**, 034302.
17. C. H. Ahn, Y. Y. Kim, D. C. Kim, S. K. Mohanta and H. K. Cho, *J. Appl. Phys.*, 2009, **105**, 013502.
18. F. Oba, A. Togo, I. Tanaka, J. Paier and G. Kresse, *Phys. Rev. B*, 2008, **77**, 245202.
19. E. V. Lavrov, J. Weber, F. Börrnert, C. G. van de Walle, and R. Helbig, *Phys. Rev. B*, 2002, **66**, 165205.
20. D. McCluskey, S. J. Jokela, K. K. Zhuravlev, P. J. Simpson and K. G. Lynn, *Appl. Phys. Lett.*, 2002, **81**, 3807.
21. D. M. Hofmann, A. Hofstaetter, F. Leiter, H. Zhou, F. Henecker, B. K. Meyer, S. B. Orlinskii, J. Schmidt and P. G. Baranov, *Phys. Rev. Lett.*, 2002, **88**, 045504.
22. C. G. Van de Walle, *Phys. Rev. Lett.*, 2000, **85**, 1012.
23. D. M. Hofmann, D. Pfisterer, J. Sann, B. K. Meyer, R. Tena-Zaera, V. Munoz-Sanjose, T. Frank and G. Pensl, *Appl. Phys. A: Mater. Sci. Proc.*, 2007, **88**, 147.
24. H. Zeng, G. Duan, Y. Li, S. Yang, X. Xu and W. Cai, *Adv. Funct. Mater.*, 2010, **20**, 2010, 561.
25. S. A. Studenikin, N. Golego and M. Cocivera, *J. Appl. Phys.*, 1998, **84**, 2287.
26. A. van Dijken, E.A. Meulenkamp, D. Vanmaekelbergh and A. Meijerink, *J. Lumin.*, 2000, **90**, 123.
27. K. Vanheusden, C. H. Seager, W. L. Warren, D. R. Tallant, J. Caruso, M. J. Hampden-Smith and T. T. Kodas, *J. Lumin.*, 1997, **75**, 11.
28. J. A. Röhr, J. Sá and S. J. Konezny, *Comm. Chem.*, 2019, **2**, 52.
29. C. H. Patterson, Phys. Rev. B, 2006, 74, 144432.
30. Y. Yang, Y. Zhang, S. Fernandez-Alberti and R. Long, J. Phys. Chem. Lett., 2024, 15, 1.
31. T. J. Penfold et al., *Nat. Comm.*, 2018, **9**, 478.
32. K. Kodama and T. Uchino, *J. Phys. Chem. C*, 2014, **118**, 23977.
33. S. B. Zhang, S. H. Wei and A. Zunger, *Phys. Rev. B*, 2001, **63**, 075205.